JOURNAL OF VIROLOGY, Aug. 2006, p. 8006–8018 Vol. 80, No. 16
0022-538X/06/$08.00+0 doi:10.1128/JVI.00743-06

Evidence for a Role of the Cellular ND10 Protein PML in Mediating Intrinsic Immunity against Human Cytomegalovirus Infections

Nina Tavalai, Peer Papior, Sabine Rechter, Martina Leis, and Thomas Stamminger*

Institut für Klinische und Molekulare Virologie der Universität Erlangen-Nürnberg, Schlossgarten 4, 91054 Erlangen, Germany

Received 12 April 2006/Accepted 30 May 2006

Several viruses, including human cytomegalovirus (HCMV), encode proteins that colocalize with a cellular subnuclear structure known as ND10. Since only viral DNA deposited at ND10 initiates transcription, ND10 structures were hypothesized to be essential for viral replication. On the other hand, interferon treatment induces an up-regulation of ND10 structures and viruses have evolved polypeptides that disperse the dot-like accumulation of ND10 proteins, suggesting that ND10 could also be part of an intrinsic defense mechanism. In order to obtain evidence for either a proviral or an antiviral function of ND10, we generated primary human fibroblasts with a stable, short interfering RNA-mediated knockdown (kd) of PML. In these cells, other ND10-associated proteins like hDaxx showed a diffuse nuclear distribution. Interestingly, we observed that HCMV infection induced the de novo formation of ND10-like hDaxx and Sp100 accumulations that colocalized with IE2 and were disrupted, in the apparent absence of PML, in an IE1-dependent manner during the first hours after infection. Furthermore, infection of PML-kd cells with wild-type HCMV at a low multiplicity of infection resulted in enhanced replication. In particular, a significantly increased plaque formation was detected, suggesting that more cells are able to support initiation of replication in the absence of PML. While there was no difference in viral DNA uptake between PML-kd and control cells, we observed a considerable increase in the number of immediate-early (IE) protein-positive cells, indicating that the depletion of PML augments the initiation of viral IE gene expression. These results strongly suggest that PML functions as part of an intrinsic immune mechanism against cytomegalovirus infections.

In addition to the conventional innate and adaptive immune responses, it was recently recognized that complex organisms have evolved a set of constitutively expressed genes that are able to repress viral infections. These so-called intrinsic immune mechanisms involve the APOBEC3 class of cytidine deaminases as well as a large family of proteins termed the TRIM family (7, 52). We were interested in determining the role of the interferon-inducible TRIM19, also known as promyelocytic leukemia protein (PML), for human cytomegalovirus (HCMV) replication. PML is essential for the integrity of a cellular subnuclear structure, termed ND10, which has been shown to colocalize with herpesvirus DNA during infection (47).

ND10 domains, also known as nuclear dots, PML nuclear bodies, or promyelocytic oncogenic domains, are spherical nuclear substructures which represent accumulations of multiple cellular proteins like Sp100, hDaxx, BLM, or SUMO-1 that require the PML protein for their formation (51). Since PML constitutes the defining component of ND10, loss of PML consequently leads to a dispersal of other ND10-associated proteins as observed in mouse PML-null fibroblasts (30, 66, 67). The PML protein was originally discovered in patients suffering from acute promyelocytic leukemia, where a reciprocal chromosomal translocation resulting in a fusion of the PML protein to the retinoic acid receptor α turned out to be responsible for this hematopoietic malignancy (13, 21, 35). Due to differential splicing of the PML gene transcript, at least seven different PML isoforms (I to VII) are expressed within cells, all sharing a common N terminus but varying in their C termini (34). Moreover, all isoforms are subject to posttranslational modifications like phosphorylation (17) or conjugation to the ubiquitin-homologous protein SUMO (SUMOylation) (36, 50). The latter modification is important for the function of PML to recruit other proteins to ND10 as clearly illustrated in case of the recruitment of hDaxx to this subnuclear structure (30).

For the ND10 components PML and hDaxx, an association with histone deacetylases, exhibiting a transcriptionally repressive function, has been demonstrated (27, 42, 65). Similarly, Sp100 also behaves as a transcriptional repressor via interaction with the heterochromatin protein HP1 (41, 60, 63). The fact that several ND10 components associate with potent repressors of gene expression gave rise to the idea of ND10 acting as sites of transcriptional repression. In contrast, however, the presence of transcriptional activators like the acetyltransferase CBP or p53 at ND10 has likewise been described previously (8, 14, 24, 39), illustrating the still-controversial debate about the role of this subnuclear structure in regulating gene expression.

Analysis of HCMV infection revealed that viral replication occurs in close association with ND10 structures, an observation which was made for several DNA viruses (29, 48). Parental HCMV genomes, for instance, show the tendency to associate with ND10 followed by the targeting of newly synthesized viral immediate-early (IE) regulatory proteins IE1-p72 (IE1) and IE2-p86 (IE2) to this subnuclear structure (2, 31). It was reported that both regulatory proteins become part of an immediate transcript environment, which evolves at ND10-associated viral genomes (31). While transiently expressed IE2

* Corresponding author. Mailing address: Institut für Klinische und Molekulare Virologie der Universität Erlangen-Nürnberg, Schlossgarten 4, 91054 Erlangen, Germany. Phone: 49 9131 852 6783. Fax: 49 9131 852 2101. E-mail: thomas.stamminger@viro.med.uni-erlangen.de.

illustrates a perfect colocalization with ND10 domains (2), the protein expressed during viral infection can also be found adjacent to these structures (4, 31, 37). At later stages of the infection cycle the development of replication compartments starting from parental genomes deposited at the periphery of ND10 domains can be observed (4). Taken together, these results implied that ND10 may play a functionally important role for the initiation of viral replication. On the other hand, however, many nuclear-replicating viruses including HCMV have evolved polypeptides which cause the disruption of ND10 early during infection (reviewed in the work of Everett [15]). IE1 of HCMV initially accumulates at ND10 sites and subsequently induces the dispersal of this subnuclear structure (2, 37, 64). As a mechanism for this, it was proposed that IE1 abrogates the SUMOylation of PML (1, 40), which would lead to a dissociation of other ND10 proteins since only SUMOylated PML is able to assemble ND10 (30, 67). In comparison to that, disruption of ND10 by the viral regulatory protein ICP0 during herpes simplex virus type 1 (HSV-1) infection is mediated through a complete degradation of SUMO-1-modified forms of PML and Sp100 in a proteasome-dependent manner (10, 16). These observations in turn have strengthened the assumption of a repressive effect of ND10 on the development of a lytic viral infection (3). In addition, many ND10 proteins are interferon inducible (11, 23), further supporting the idea of ND10 being part of an antiviral defense mechanism of the cell. Thus, the functional consequences of the tight association of viral genomes and proteins with ND10 domains are still controversial.

To further clarify the role of ND10 for HCMV replication, we generated primary human foreskin fibroblasts (HFFs) with a knockdown of PML (PML-kd). PML was chosen since this protein has previously been shown to be essential for the integrity of ND10 (30). Depletion of PML resulted in a microdispersed nuclear localization of ND10 constituents like Sp100 or hDaxx, which were, however, reorganized into ND10-like complexes after HCMV infection. Functional analysis of HCMV replication in PML-deficient cells revealed an enhanced viral replication in the absence of PML that was found to be due to a higher number of cells initiating IE gene expression. Our results underline the notion that PML and/or ND10 domains function as part of an intrinsic antiviral defense mechanism of the cell by repressing viral IE gene expression.

MATERIALS AND METHODS

Plasmid constructions. The sequences of oligonucleotides used for PCR, plasmid constructions, and sequencing are available as supplementary data (available upon request by contacting the author). The expression plasmid for myc-tagged PML was constructed by excision of the coding sequence for PML isoform VI from plasmid pAS-PML (30) via NcoI and BamHI followed by a filling-in reaction with Klenow enzyme and insertion into the EcoRV site of plasmid myc-pcDNA3 (25). The plasmid encoding FLAG-tagged pUL69 was described previously (44). Plasmid pHM990 for IE2-p86 fused to enhanced green fluorescent protein (EGFP) was generated by PCR amplification of the IE2-p86 cDNA followed by insertion into plasmid pEGFP-N1 via BglII and Asp718. Plasmid pHM2396, encoding a fusion protein of the monomeric red autofluorescent protein mCherry with PML isoform VI, was constructed by PCR amplification of the mCherry coding sequence using primers 5′- and 3′mCherry together with plasmid pRSET-B-mCherry as template (61). In parallel, the coding sequence for PML isoform VI was amplified with primers 5′- and 3′PMLm-Cherry. Finally, primers 5′mCherry/BamHI-PML and 3′PML/SacII-mCherry were used for a hybrid PCR to generate the fusion gene which was then inserted via BamHI and SacII into the pLenti6/V5-D-Topo vector (Invitrogen, Karlsruhe, Germany). For generation of plasmid pHM2421, carrying an mCherry/PML fusion gene that is resistant against silencing by short interfering RNA (siRNA) siPML2, a 5-nucleotide change of the PML sequence was introduced by site-directed mutagenesis using primers 5′PML-R and 3′PML-R. Site-directed mutagenesis was performed as described previously (43).

Cell culture, transfections, and virus infections. HFF cells were prepared from human foreskin tissue as described previously (33). HFFs and HEK293T and 293FT cells were cultured and transfected as described previously (25). Infection experiments were performed either with the laboratory HCMV strain AD169, the recombinant HCMV AD169-GFP (expressing green fluorescent protein) (46), or the IE1 deletion mutant CR208 (kindly provided by R. Greaves and E. Mocarski) (22). Virus titers for HCMV AD169 and AD169-GFP were determined by IE1p72-fluorescence as described previously (5). Briefly, HFFs were infected with various dilutions of virus stocks. After 24 h of incubation, cells were fixed and stained with monoclonal antibody p63-27 directed against IE1p72 (5). Subsequently, the number of positive cells was determined and used to calculate viral titers (indicated in IE protein-forming units [IEU]). Virus titers of CR208 (virus stock kindly provided by M. Nevels) were determined as described previously (53). For viral growth analysis, the replication of HCMV AD169-GFP was quantified by automated fluorometry as described previously (46). Plaque assays were performed by infection of HFFs (3.0×10^5) in six-well plates with the indicated amount of virus. One hour postinfection (hpi) the virus supernatant was removed and overlay medium was added to the cells followed by incubation for 7 days until the number of plaques was determined.

RNAi. Target sequences for RNA interference (RNAi) were selected using siRNA Designer software (BD Biosciences, Heidelberg, Germany). The target sequence siDaxx1 against hDaxx has been published previously (12). Additional siRNA sequences were as follows: siDaxx2, GACGATGAGGAGAGTGATG (targeting codons 473 to 479 of hDaxx); siPML1, AGAGTCGGCCGACTT CTGG (targeting codons 132 to 139 of PML); siPML2, AGATGCAGCTGTA TCCAAG (targeting codons 394 to 400 of PML); siLuci, GTGCGTTGCTAGT ACCAAC (targeting luciferase). Oligonucleotides for short hairpin RNAs (shRNAs) were designed with the siRNA Hairpin Oligonucleotide Sequence Designer Tool (BD Biosciences) and contained (5′ to 3′) a BamHI site, the respective siRNA sequence, a loop region, the complementary siRNA sequence, an RNA polymerase III termination sequence, a NheI site, and an EcoRI cloning site. In the siC oligonucleotide, which served as a negative control, no complementary sequence was incorporated. Double-stranded oligonucleotides were inserted either into the retroviral vector pSIREN-RetroQ (BD Biosciences) or into vector pSIREN-RetroQ-IRES-EGFP (kindly provided by F. Neipel, Erlangen, Germany), which was modified by insertion of an internal ribosome entry site (IRES)-EGFP expression cassette downstream of puromycin. The correct sequence of cloned shRNA oligonucleotides was confirmed by automated sequencing using primers U6 forward and SirenRetroQ78R. The respective plasmids, which were designated according to their inserted siRNA sequence, were used either for transfection experiments or for retrovirus transduction.

Retrovirus transduction and selection of stably transduced cells. Replication-deficient, murine leukemia virus-based retroviruses were prepared by cotransfection of 293FT cells (Invitrogen) with pSIREN-RetroQ plasmids together with packaging plasmids pHIT60 (kindly provided by K. Überla, Bochum, Germany) and pVSV-G (Invitrogen) using the Lipofectamine 2000 reagent (Invitrogen). Viral supernatants were harvested 48 h after transfection, clarified by centrifugation, filtered, and stored in aliquots at −80°C. Low-passage-number primary HFF cells were incubated for 24 h with retrovirus supernatants in the presence of 7.5 μg/ml of Polybrene (Sigma-Aldrich, Deisenhofen, Germany). Then, puromycin was added (0.5 to 5 μg/ml) to the cell culture medium in order to select a stably transduced cell population. For all experiments, control cell cultures were prepared in parallel using control retroviruses expressing either no siRNA (vector) or a nonfunctional siRNA (siC). For each siRNA expression construct at least two cell populations were generated independently with different batches of primary HFF cells. PML was reintroduced into siPML2-expressing cells via retrovirus transduction and blasticidin selection using the ViraPower lentivirus expression system with the coding sequence of PML (isoform VI) fused to the autofluorescent protein mCherry cloned into the pLenti6/V5-D-Topo vector (Invitrogen).

Real-time PCR. For real-time PCR, DNA was extracted from virus-infected cells using the DNeasy tissue kit (QIAGEN, Hilden, Germany). Real-time PCR was performed as described previously (45) with the following exceptions: reactions were performed in a 20-μl reaction mixture containing 2.5 μl of either the sample or the standard DNA solution, 10 μl 2× TaqMan PCR Mastermix (Applied Biosystems), 7.5 pmol of each primer, and 5 pmol probe. The HCMV-specific primer and probe sequences were described previously (45). Primers

(5′Alb, GTGAACAGGCGACCATGCT; 3′Alb, GCATGGAAGGTGAATGT TTCAG) and a 6-carboxyfluorescein–6-carboxytetramethylrhodamine-labeled probe (TCAGTGGAAGATGAAACATACGTTC) against the cellular albumin gene were used to quantify cellular DNA, thus facilitating the calculation of the ratio of viral DNA/cell. For each sample, DNA extracts were analyzed in triplicate.

Antibodies, indirect immunofluorescence, and Western blot analysis. For detection of endogenous PML protein, the monoclonal antibodies 5E10 (kindly provided by Roel van Driel) (62) and PG-M3 (Santa Cruz Biotechnology, Santa Cruz, Calife.) and the polyclonal rabbit serum H-238 (Santa Cruz Biotechnology) were used. hDaxx was detected by the rabbit polyclonal antiserum M-117 (Santa Cruz Biotechnology) and the murine monoclonal antibody MCA2143 (Serotec, Oxford, United Kingdom). Polyclonal rabbit serum H-60 (Santa Cruz Biotechnology) was used for visualization of Sp100. Antibodies to IE1 (p63-27) and IE2 (anti-pHM178 and anti-SMX) have been described previously (5, 25, 54). Monoclonal antibodies anti-FLAG M2 and anti-actin (Sigma-Aldrich) were used for control reactions.

For indirect immunofluorescence analysis primary HFF cells (3×10^5) were grown on coverslips for transient transfection or HCMV infection, respectively. The conditions for transfection of HFFs, as well as for fixation and immunodetection of viral and cellular proteins, were as described previously with the exception that Alexa 488- or Alexa 555-conjugated secondary antibodies (Molecular Probes) were used (26).

For Western blotting, extracts from transfected, transduced, or infected cells were prepared in sodium dodecyl sulfate loading buffer, separated on sodium dodecyl sulfate-containing 8 to 15% polyacrylamide gels, and transferred to nitrocellulose membranes. Western blotting and chemiluminescence detection were performed as described previously (44).

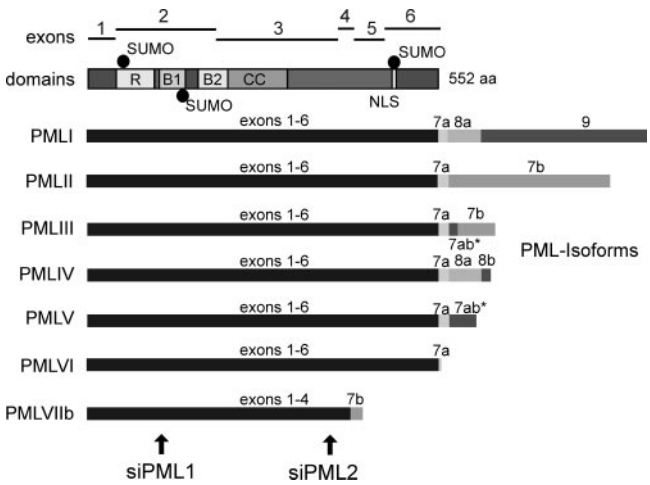

FIG. 1. Localization of target sequences for siRNAs against PML relative to the localization of exons and protein domains (data taken from reference 34). All PML isoforms share a common N terminus but differ in their C termini due to alternative usage of 3′ exons. Protein domains of PML are given in the upper part of the figure. R, RING finger; B1 and B2, B boxes; CC, coiled-coil domain; SUMO, SUMOylation sites. The lower part illustrates the exon assembly of various PML isoforms. Positions within PML that are targeted by the siRNAs siPML1 and siPML2 are indicated by arrows.

RESULTS

Generation of primary human fibroblasts with a stable knockdown of PML. In order to further clarify the role of ND10 domains for HCMV replication, we decided to generate cells which are devoid of ND10. Since PML has previously been shown to be essential for the accumulation of ND10 proteins (30), we selected two different siRNA sequences, termed siPML1 and siPML2, that target the coding sequence of all known PML isoforms and should thus be able to knock down PML gene expression (Fig. 1). These sequences, together with other siRNA sequenced that were used as controls (siC, siLuci, siDaxx1, and siDaxx2), were cloned into the retroviral siRNA expression vector pSIREN-RetroQ, which facilitates RNAi-mediated knockdown via the stable expression of shRNAs that are further processed into siRNAs. In addition, we used a modified pSIREN-RetroQ vector (pSIREN-RetroQ-IRES-EGFP) containing an expression cassette for enhanced green fluorescent protein, thus allowing the easy detection of either transfected or transduced cells. Then, the efficacy of the selected siRNAs against PML was tested in transient-transfection experiments: this revealed that siPML2 is able to induce a highly efficient and specific knockdown of PML whereas siPML1 is considerably less effective (data not shown).

In a next step, primary HFFs with a stable knockdown of PML gene expression should be generated. In a first series of experiments, HFFs were transduced with retrovirus vectors expressing either the PML-specific siRNAs siPML1 and siPML2 or various control siRNAs; both vectors, pSIREN-RetroQ and pSIREN-RetroQ-IRES-EGFP, were used for transduction experiments. After selection of puromycin-resistant cell populations, the knockdown of endogenous PML was analyzed by Western blotting. As shown in Fig. 2A, anti-PML monoclonal antibody 5E10 detected a major signal of approximately 130 kDa as well as several additional signals which corresponded to the various SUMOylated and non-SUMOylated isoforms of PML (34). As already observed in transient expression experiments, siPML1 induced only a partial silencing (Fig. 2A, lanes 4 and 11), whereas expression of siPML2 resulted in a complete down-regulation of PML (Fig. 2A, lanes 5 and 12). The potency of siPML2 was confirmed in a second series of experiments with independently transduced cells: again, siPML2 expression resulted in an apparently complete knockdown of all PML isoforms as detected by Western blot analysis with both monoclonal antibody 5E10 (Fig. 2B, lanes 1 to 3, upper panel) and a polyclonal serum against PML (Fig. 2B, lanes 4 to 6, upper panel). However, we cannot rule out a small amount of residual PML. In contrast, beta-actin and hDaxx levels were not affected by siPML2 (Fig. 2B, lower panels). As assessed by indirect immunofluorescence analysis, more than 95% of the siPML2 cell population showed a knockdown of PML (data not shown). Thus, we were able to generate primary human fibroblasts in which PML protein levels were highly suppressed.

Depletion of PML induces a dissociation of hDaxx and Sp100. Since PML was reported to be essential for the integrity of ND10 domains (30), we were interested to investigate the subcellular localization of the other major ND10 components, hDaxx and Sp100, in the generated PML-kd cells. Consistent with previous observations for $PML^{-/-}$ mouse primary embryonic fibroblasts (30), indirect immunofluorescence analysis of the PML-kd cells revealed that both hDaxx and Sp100 were no longer present in a punctate staining pattern in the absence of PML but could be observed in a diffuse, microdispersed nuclear localization (Fig. 3C, subpanels c and g). In control HFFs, which were generated in parallel, the distribution of PML, Sp100, and hDaxx showed the typical costaining in ND10 punctate structures, indicating that neither the expression of nonrelated siRNAs nor the retrovirus transduction and puromycin selection of cells affected ND10 morphology (Fig. 3A and B). Interestingly, we observed that, although the overall

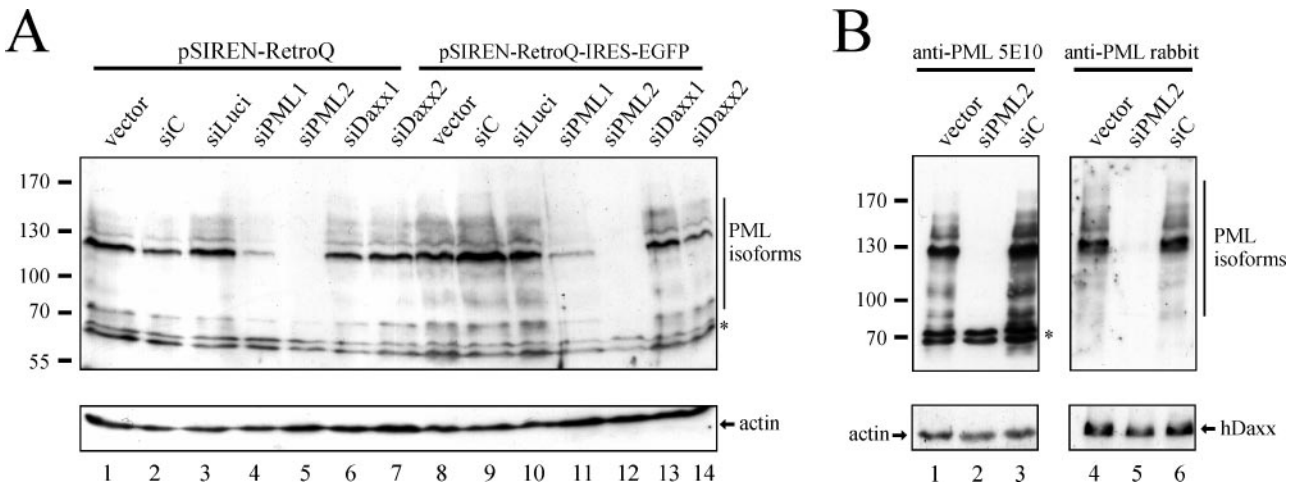

FIG. 2. Detection of endogenous PML by Western blot analysis of cell lysates derived from primary human fibroblasts transduced with various siRNA expression vectors as indicated. (A) Upper panel: monoclonal anti-PML antibody 5E10 was used to detect PML; lower panel: beta-actin was detected as a loading control. (B) Comparison of the reactivities of anti-PML monoclonal antibody 5E10 and anti-PML rabbit serum H-238 using cell lysates from primary human fibroblasts transduced with pSIREN-RetroQ vectors as indicated. Lanes 1 to 3, upper panel: monoclonal 5E10; lower panel: beta-actin antibody. Lanes 4 to 6, upper panel: anti-PML rabbit serum H-238; lower panel: anti-Daxx rabbit serum M-117. The localization of PML isoforms is indicated on the right of each panel; the asterisks indicate a nonspecific reaction of anti-PML antibody 5E10. Numbers at left of each panel are molecular masses in kilodaltons.

patterns of Sp100 and hDaxx staining were rather similar in PML-kd cells, both proteins no longer colocalized, indicating that they dissociate to different subnuclear sites in the absence of PML (Fig. 3C, subpanels k, l, and m).

Diffuse distribution of IE2 after transient expression in PML knockdown cells. It has previously been demonstrated that the major regulatory protein IE2-p86 (IE2) of HCMV exhibits a tight spatial association with ND10 domains. While dot-like accumulations of transiently expressed IE2 display a perfect ND10 colocalization (2), the viral IE protein can be found both colocalizing and adjacent to this subnuclear structure during HCMV infection (4, 31, 37). Since the cellular proteins responsible for the recruitment of IE2 to ND10 domains are not known, we were interested to investigate the subnuclear distribution of IE2 in the apparent absence of PML. For this, PML-depleted primary HFFs as well as control fibroblasts were transfected with plasmid pHM990 expressing an EGFP-tagged version of IE2-p86. Subsequently, indirect immunofluorescence analyses were carried out using anti-PML, anti-hDaxx, or anti-Sp100 antibodies to detect the endogenous ND10 proteins. Interestingly, this experiment revealed that the punctate association of IE2 with PML, as detected after transfection of control fibroblasts (Fig. 4A), changed to an exclusively diffuse distribution of the viral regulatory protein in PML-kd cells (Fig. 4B). The dot-like localization of transiently expressed IE2 is therefore dependent on the presence of PML or intact PML-associated nuclear bodies. Furthermore, in case of dispersed ND10 structures as observed in PML-depleted cells, the diffusely distributed IE2 protein could no longer be found in any apparent spatial association with other ND10 components like hDaxx or Sp100 (Fig. 4B, subpanels d and h).

Dot-like accumulation of IE2 after infection of PML knockdown cells and colocalization with reorganized ND10-like structures. Having shown that the subcellular distribution of transiently expressed IE2 is altered into a diffuse pattern in the absence of ND10 domains, we next asked whether this is also the case during HCMV infection. To determine the effect of dispersed ND10 structures on the intracellular distribution of IE2, PML-depleted as well as control fibroblasts were infected with wild-type HCMV (AD169) at a multiplicity of infection (MOI) of 1. Samples were harvested at the indicated time points after infection for immunofluorescence analyses utilizing anti-PML, anti-hDaxx, or anti-Sp100 antibodies for the detection of the endogenous ND10 components (Fig. 5). Surprisingly, in contrast to the results obtained in transient-transfection experiments, the dispersal of ND10 had no influence on the dot-like accumulation of IE2 in the context of HCMV infection. IE2 was still observable in characteristic discrete intranuclear foci from 2 hpi up to 24 hpi (Fig. 5A and C, subpanels b, f, and k) in a manner similar to that observed after infection of PML-positive cells (data not shown). This result led us to the conclusion that PML and ND10 are not necessary for the subnuclear dot-like accumulation of IE2 during infection.

The analysis of the subcellular distribution of Sp100 and hDaxx during HCMV infection of PML-depleted cells resulted in an additional interesting finding: during the first 2 to 3 h of HCMV infection, a reaggregation of diffusely distributed hDaxx and Sp100 into distinct nuclear substructures, resembling ND10 domains, was detectable in PML-kd cells (Fig. 5A, subpanels c, g, and l, and 5B, subpanel g; infected cells are indicated by arrows). Moreover, for the IE2 protein an association with these newly formed ND10-like structures consisting of either Sp100 or hDaxx could be demonstrated (Fig. 5A, subpanels b to d, f to h, and k to m, and 5B, subpanels f to h; compare infected, IE2-positive cells with noninfected, IE2-negative cells). The observation that the IE2 protein colocalizes with punctate foci of both cellular proteins indicates that Sp100 and hDaxx, which were found at distinct subnuclear sites

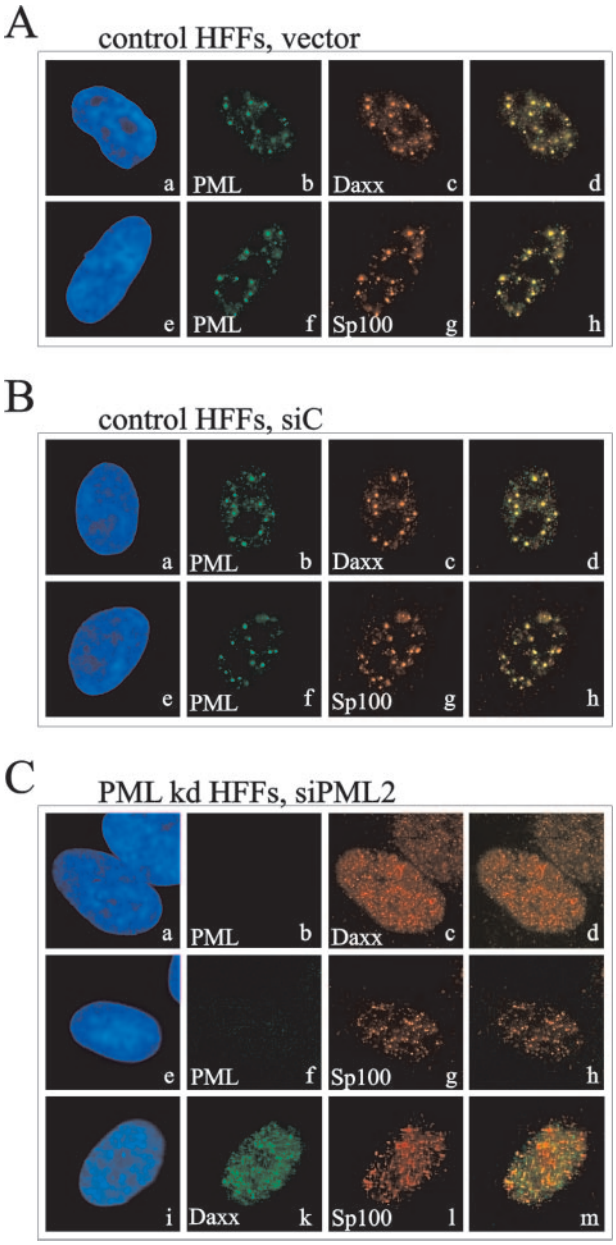

FIG. 3. Stable knockdown of PML in primary human fibroblasts leads to a dispersal of ND10 domains with a dissociation of hDaxx and Sp100. The figure shows detection of ND10 structures in primary human fibroblasts stably transduced with various siRNA vectors by indirect immunofluorescence analysis. The following antibodies were used for staining: anti-PML monoclonal antibody PG-M3 (b and f), anti-hDaxx polyclonal serum M-117 (c), and anti-Sp100 polyclonal serum H-60 (g); the costaining in panel C, subpanels i to m, was performed using anti-hDaxx monoclonal antibody MCA2143 (k) together with anti-Sp100 serum H-60 (l). DAPI (4′,6′-diamidino-2-phenylindole) staining of the respective cell nuclei is shown in subpanels a, e, and i; subpanels d, h, and m show merged images of PML/hDaxx, PML/Sp100, or hDaxx/Sp100 staining, respectively. (A) pSIREN-RetroQ-transduced control HFFs. (B) pSIREN-RetroQ-siC-transduced control fibroblasts. (C) pSIREN-RetroQ-siPML2-transduced PML-kd fibroblasts.

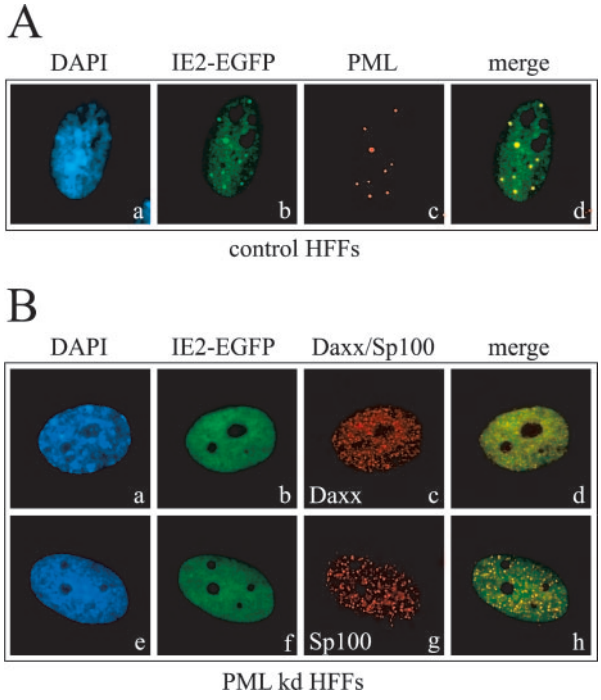

FIG. 4. Localization of IE2-p86 after transient expression in PML knockdown or control fibroblasts. Control HFFs (A) or siPML2-expressing PML-kd fibroblasts (B), grown on coverslips, were transfected with a eukaryotic expression vector encoding IE2-p86 fused to EGFP. Thereafter, indirect immunofluorescence analyses were carried out. IE2-p86 was detected via EGFP autofluorescence (A, subpanel b; B, subpanels b and f); endogenous ND10 proteins were visualized via anti-PML monoclonal antibody PG-M3 (A, subpanel c) or via the polyclonal rabbit sera M-117 against hDaxx (B, subpanel c) and H-60 against Sp100 (B, subpanel g). DAPI, 4′,6′-diamidino-2-phenylindole.

in noninfected PML-kd cells (Fig. 3C), apparently reassociate in the context of HCMV infection. We conclude that the ablation of PML did not eliminate the potential of other ND10 components like Sp100 or hDaxx to become associated with at least a subset of IE2 accumulations. However, this relocalization of Sp100 and hDaxx to distinct nuclear aggregates was only transitory, since at later stages of the replication cycle (12 to 24 hpi) both cellular proteins showed a micropunctate staining pattern again (Fig. 5C; data not shown for Sp100). Comparable to the situation in control fibroblasts, the dispersal of the reorganized ND10-like structures had no influence on IE2 localization, as the viral regulatory protein retained its dot-like distribution (Fig. 5C, subpanels b and f).

IE1-induced dispersal of reorganized, ND10-like accumulations of Sp100 and hDaxx in the absence of PML. Since the dispersal of reorganized, ND10-like accumulations of Sp100 and hDaxx in PML-kd cells resembled the kinetics of IE1-mediated disruption of genuine ND10 (2), we were interested to determine whether IE1 might be responsible for this. It has previously been reported that IE1 transiently colocalizes with ND10 during the first 2 to 3 h after infection, which is then followed by a rapid redistribution of both PML and IE1 into a nuclear diffuse form (2, 37). Furthermore, Ahn and colleagues postulated that disruption of ND10 by IE1 is mediated via a direct protein interaction with PML (1). First, we wanted to determine the subcellular localization of IE1 in the apparent absence of PML. For this, PML-kd and control fibroblasts were infected with HCMV followed by indirect immunofluorescence detection of IE1, PML, or hDaxx during the first 3 hpi

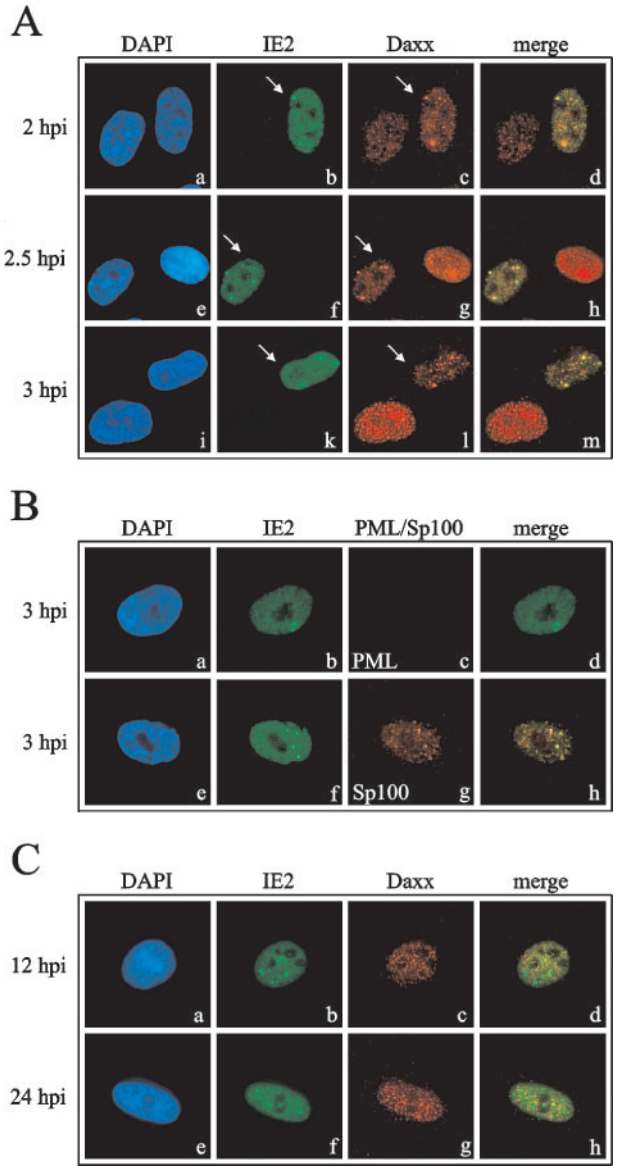

FIG. 5. Analysis of the intranuclear localization of IE2 and cellular ND10 proteins in PML knockdown cells after infection with wild-type HCMV (AD169). (A and B) Subnuclear localization of IE2 together with hDaxx (A) or PML/Sp100 (B) during the first 2 to 3 hpi of PML-kd cells. Arrows in panel A indicate HCMV-infected cells. IE2 was detected by monoclonal antibody SMX; hDaxx, PML, or Sp100 was detected by polyclonal antiserum M-117, H-238, or H-60, respectively. IE2 is detectable in punctate foci which colocalize with reorganized ND10-like structures containing hDaxx (A; compare infected with noninfected cells) and Sp100 (B). (C) Subnuclear localization of IE2 and hDaxx at 12 or 24 hpi. IE2 was detected by monoclonal antibody SMX; hDaxx was stained using polyclonal serum M-117.

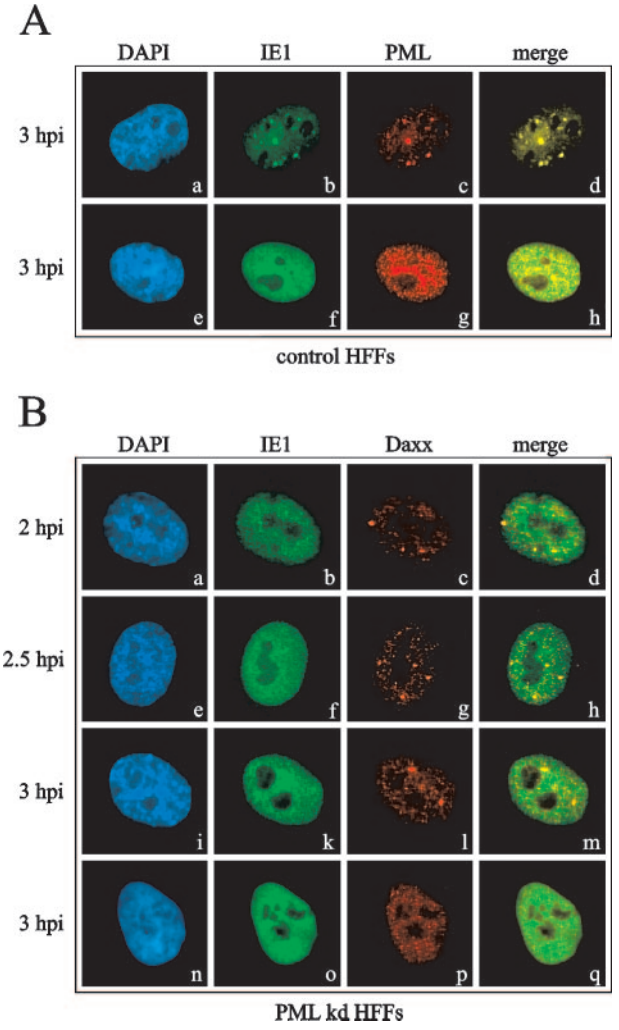

FIG. 6. Analysis of the subcellular localization of IE1 and the ND10 components PML and hDaxx during the time course of infection in PML-kd and control fibroblasts. Control fibroblasts, transduced with pSIREN-RetroQ (A), and siPML2-transduced cells (B) grown on coverslips were infected with AD169 at an MOI of 1 and harvested during the first hours postinfection as indicated. Indirect immunofluorescence analysis was performed to investigate the intranuclear localization of IE1, hDaxx, and PML by utilization of the anti-IE1 antibody p63-27 as well as the polyclonal antisera H-238 and M-117 for detection of PML and hDaxx, respectively. DAPI, 4′,6′-diamidino-2-phenylindole.

(Fig. 6). At 3 h after infection of control fibroblasts, approximately half of the cells still exhibited a punctate, PML-associated IE1 distribution, whereas in the remaining cells IE1 together with PML was already in a diffuse form (Fig. 6A). In contrast, all PML-kd cells infected with HCMV showed a diffuse staining pattern for IE1, even when earlier time points were examined (Fig. 6B, subpanels b, f, k, and o). This indicates that PML is indeed required for the punctate distribution pattern of IE1 during the first 2 to 3 h after infection. However, during our time course analysis we could observe that dot-like hDaxx accumulations, which were induced after HCMV infection of PML-kd cells, started to be redistributed into a diffuse pattern at 3 hpi (Fig. 6B, subpanels c, g, l, and p), suggesting that IE1 may still exert its activity to dissolve ND10 protein accumulations, even in the absence of PML. In order to further prove this, infection experiments were performed with the IE1 deletion mutant CR208 (22). Consistent with previous reports, this virus, lacking IE1, was no longer able to redistribute ND10 domains as could be observed after infection of control fibroblasts (Fig. 7A) (1). Interestingly, the reorganized, ND10-like accumulations of hDaxx and Sp100 also persisted after infection of PML-kd cells with CR208 and could be detected in

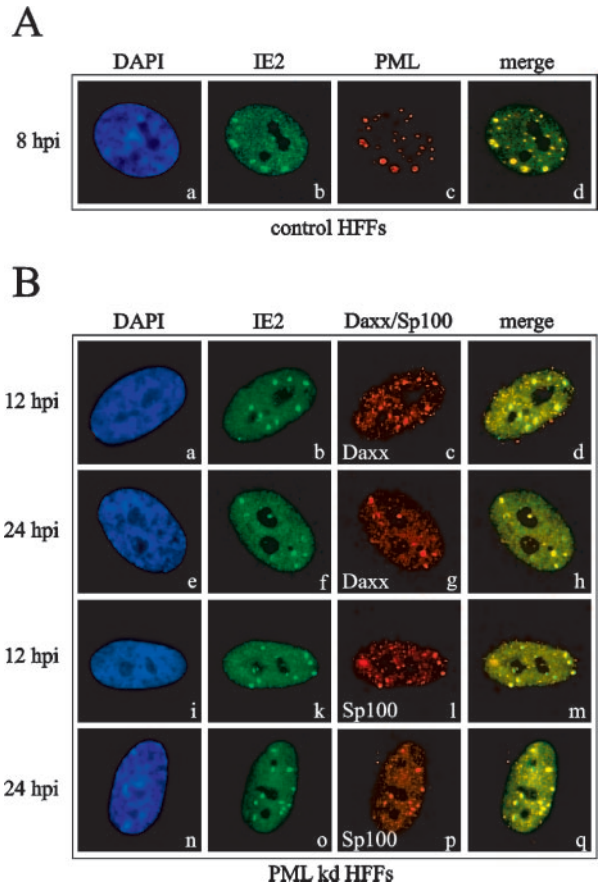

FIG. 7. Subnuclear distribution of PML, hDaxx, and Sp100 in PML-deficient and control cells infected with the IE1 deletion virus CR208. Control HFFs, transduced with pSIREN-RetroQ (A), and siPML2-transduced PML-kd cells (B) grown on coverslips were infected with the IE1 mutant virus CR208 at an MOI of 1. In subsequent immunofluorescence experiments the formation of distinct PML, hDaxx, and Sp100 foci was examined at the indicated time points after infection using the anti-PML antibody PG-M3, the anti-Daxx antibody MCA2143, and the anti-Sp100 antiserum H-60. Infected cells were identified by staining of the IE2 protein with the monoclonal antibody SMX (B, subpanels k and o) or the polyclonal antiserum pHM178 (A, subpanel b; B, subpanels b and f). DAPI, 4′,6′-diamidino-2-phenylindole.

colocalization with IE2 punctate structures up to 24 hpi. This strongly suggests that IE1 is responsible for the dispersion of reorganized ND10-like structures in PML-kd cells.

Enhanced replication of HCMV after low-MOI infection of PML knockdown cells. Next, we wanted to investigate whether the depletion of PML from primary human fibroblasts affects the efficacy of HCMV replication in general. In a first series of experiments, PML knockdown fibroblasts together with control fibroblasts were infected with the recombinant HCMV AD169-GFP. This virus contains an EGFP expression cassette inserted within the U_S gene region of HCMV strain AD169 and has previously been shown to facilitate a highly reproducible monitoring of viral replication via GFP visualization and quantification (46). In the experiment shown in Fig. 8A, control cells and PML-kd cells were infected at an MOI of 0.02 followed by GFP visualization at day 10 after infection: significantly more GFP fluorescence was observed in infected PML knockdown cells than in the control cells, indicating enhanced replication of HCMV in the absence of PML (Fig. 8A). This could also be detected by GFP quantification via automated fluorometry, which was performed during a time course analysis of 10 dpi (Fig. 8B).

In order to confirm these results obtained with the recombinant HCMV AD169-GFP, we initiated a second series of experiments using the laboratory strain AD169 of HCMV. As an alternative experimental approach, a standard plaque assay was performed in order to quantify HCMV replication. Control cells and PML knockdown cells were infected in parallel with either 5, 10, 20, 50, or 100 IEU per well. Seven days after infection the number of plaques was determined. As shown in Fig. 8C, we observed an approximately fourfold-higher number of plaques after infection of two different PML-kd cell populations expressing siPML2 than after infection of the control cells (Fig. 8C; compare siPML2 and siPML2-EGFP with vector, siC, vector-EGFP, and siC-EGFP). This result suggested that more cells are able to initiate viral replication after infection of PML-depleted cells at a low MOI.

In order to analyze whether this could be due to an increased viral uptake of PML-kd cells, we infected siPML2-expressing and control HFFs with HCMV AD169 at an MOI of 0.02. Then, 24 h later, DNA was extracted, followed by real-time PCR quantification of HCMV DNA as well as of the cellular albumin gene, which was used as a standard for calculating cell numbers. As shown in Fig. 8D, no significant difference between the viral DNA load of PML-kd cells and that of the control cells was detected, indicating that viral uptake is not altered in the absence of PML.

More cells initiate viral IE gene expression in the absence of PML. The experiments described above strongly suggested that the depletion of PML from primary human fibroblasts facilitates the initiation of HCMV gene expression, thus leading to a higher number of infected cells. To further prove this, we analyzed whether viral IE gene expression is increased in the absence of PML. For this, PML-kd and control cells were infected with 100 IEU/well of HCMV strain AD169. Twenty-four hours later, cells were immunostained for IE1 and the number of IE1-expressing cells was determined. Consistent with the results obtained by plaque assays, we observed an approximately fourfold-higher number of cells expressing IE1 (Fig. 9A) or IE2 (data not shown) protein after infection of PML knockdown cells than after infection of the control cells (Fig. 9A). This was also reflected by an increased amount of IE1 and IE2 protein after infection with a low MOI as detected by Western blot experiments with cell lysates harvested at various times after infection (Fig. 9B, lane 6, and C, lanes 6 and 9). Since it was suggested that the IE1 protein may be able to counteract a potential antiviral effect of ND10 domains, we were also interested to investigate replication of the IE1 deletion mutant CR208 in PML-deficient cells. As shown in Fig. 9D, infection of PML-kd cells with CR208 resulted in approximately 20-fold-more IE2-positive cells than among the control cells, suggesting an even stronger effect of PML depletion in the absence of IE1. Furthermore, in contrast to wild-type HCMV, increased IE gene expression could be detected under both low- and high-MOI conditions with CR208 as analyzed by Western blotting experiments (Fig. 9E). In summary, we conclude that depletion of PML from primary human HFFs aug-

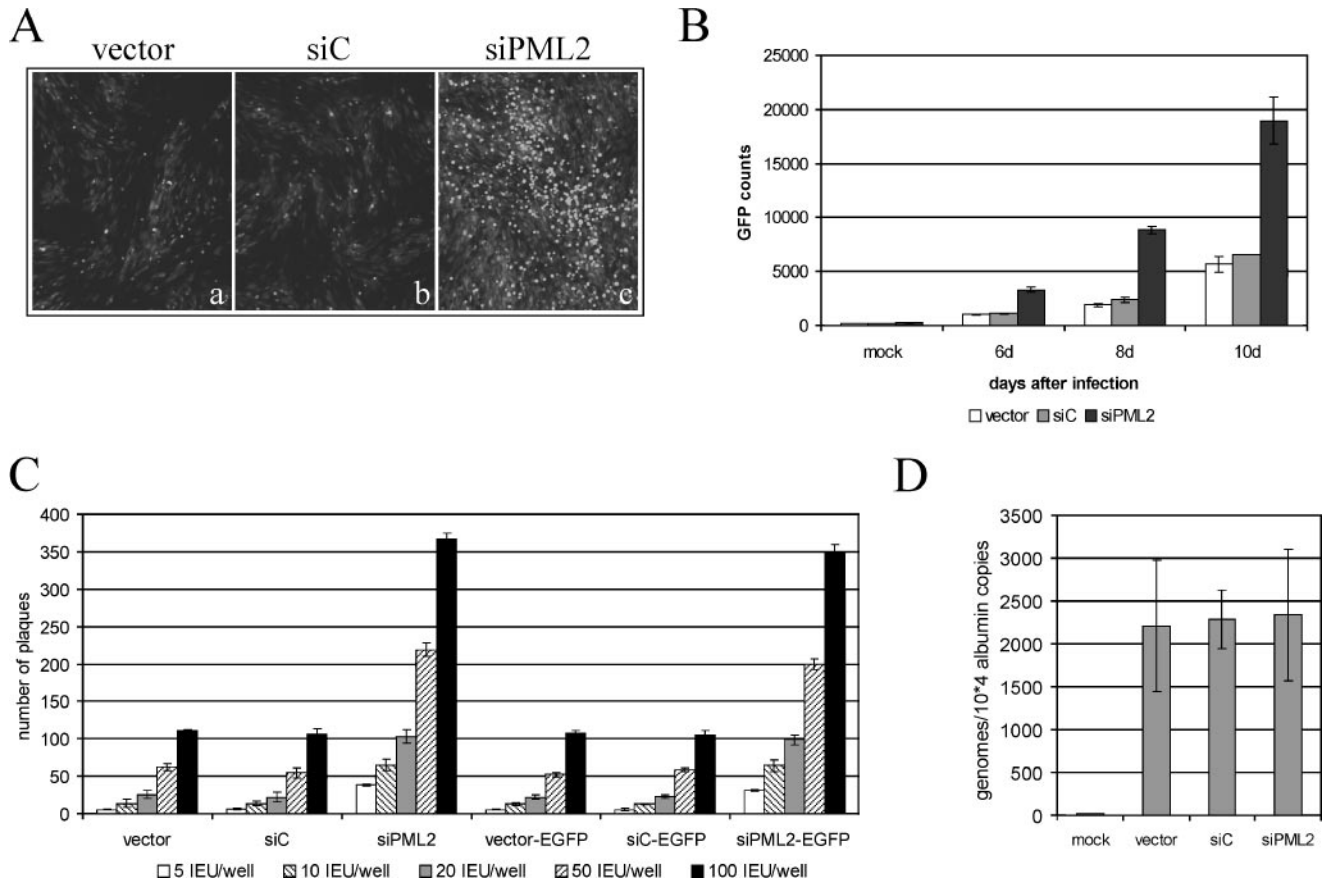

FIG. 8. Quantification of HCMV replication in retrovirally transduced HFFs expressing siRNAs. (A and B) Retrovirally transduced HFFs (vector, siC, and siPML2) were infected with recombinant HCMV AD169-GFP expressing green fluorescent protein. Panel A shows the GFP fluorescence 10 days after infection of the indicated HFFs (MOI of 0.02). Panel B shows a quantification of the GFP fluorescence by automated fluorometry at days 6, 8, and 10 after infection with HCMV AD169-GFP. (C) Quantification of the number of plaques by standard plaque assays 7 days after infection of transduced HFFs (vector, siC, siPML2, vector-EGFP, siC-EGFP, and siPML2-EGFP) with the indicated amount of HCMV strain AD169 (viral inoculum ranging from 5 to 100 IEU of virus per well of a six-well dish). (D) Quantitative real-time PCR for evaluation of the viral DNA load after infection of PML-kd cells in comparison to control fibroblasts. HFF cells as indicated were infected with AD169 at an MOI of 0.02. Then, DNA was extracted 24 hpi and the number of HCMV genome copies was determined by real-time PCR. The amplification of the cellular albumin gene was utilized as a standard for calculating the cell numbers.

ments the initiation of HCMV IE gene expression, suggesting that PML acts as a repressor of viral IE gene expression.

Reintroduction of PML isoform VI into siPML2-expressing cells reverses enhanced HCMV IE gene expression. Since our results concerning enhanced HCMV replication critically depended on the depletion of PML by one specific siRNA, we wanted to make sure that no off-target RNAi effects contribute to the observed phenotype of siPML2-expressing HFFs. Therefore, we decided to reintroduce PML into siPML2-expressing cells. In order to facilitate the detection of reintroduced PML, we generated an N-terminal fusion gene of PML, isoform VI, with the monomeric autofluorescent protein mCherry (61) in the context of the retroviral vector pLenti6/V5-D-Topo, termed mCh-PML. Furthermore, silent mutations were inserted into the target sequence of siPML2 by site-directed mutagenesis, resulting in plasmid mCh-PML-R. In order to verify that mCh-PML-R could no longer be silenced by siPML2, transient expression experiments were performed. HEK293T cells were cotransfected with either mCh-PML or mCh-PML-R plasmids and various pSIREN-RetroQ-based shRNA expression vectors as well as with an expression vector for FLAG-tagged pUL69 followed by Western blot analysis of PML and pUL69 (Fig. 10A). While expression from mCh-PML was still efficiently down-regulated (Fig. 10A, lane 7), mCh-PML-R protein levels were not affected after cotransfection with siPML2, thus confirming the expression of a silencing-resistant form of PML (Fig. 10A, lane 9). We then went on to transduce siPML2 HFFs with retroviral vectors for either mCh-PML or mCh-PML-R followed by incubation in the presence of blasticidin in order to select stably transduced cell populations. Immunofluorescence analysis revealed that both mCh-PML- and mCh-PML-R-transduced cells were positive for PML, as detected by mCherry autofluorescence. However, whereas mCh-PML-R-expressing HFFs contained large, unphysiological PML dots, as also observed after overexpression of PML in transient-transfection experiments (data not shown), mCh-PML-transduced cells exhibited punctate PML accumulations that colocalized with hDaxx and Sp100, thus indicating the successful reorganization of ND10 in siPML2 cells that overexpress the nonmutated mCh-PML (Fig. 10B). Western blot anal-

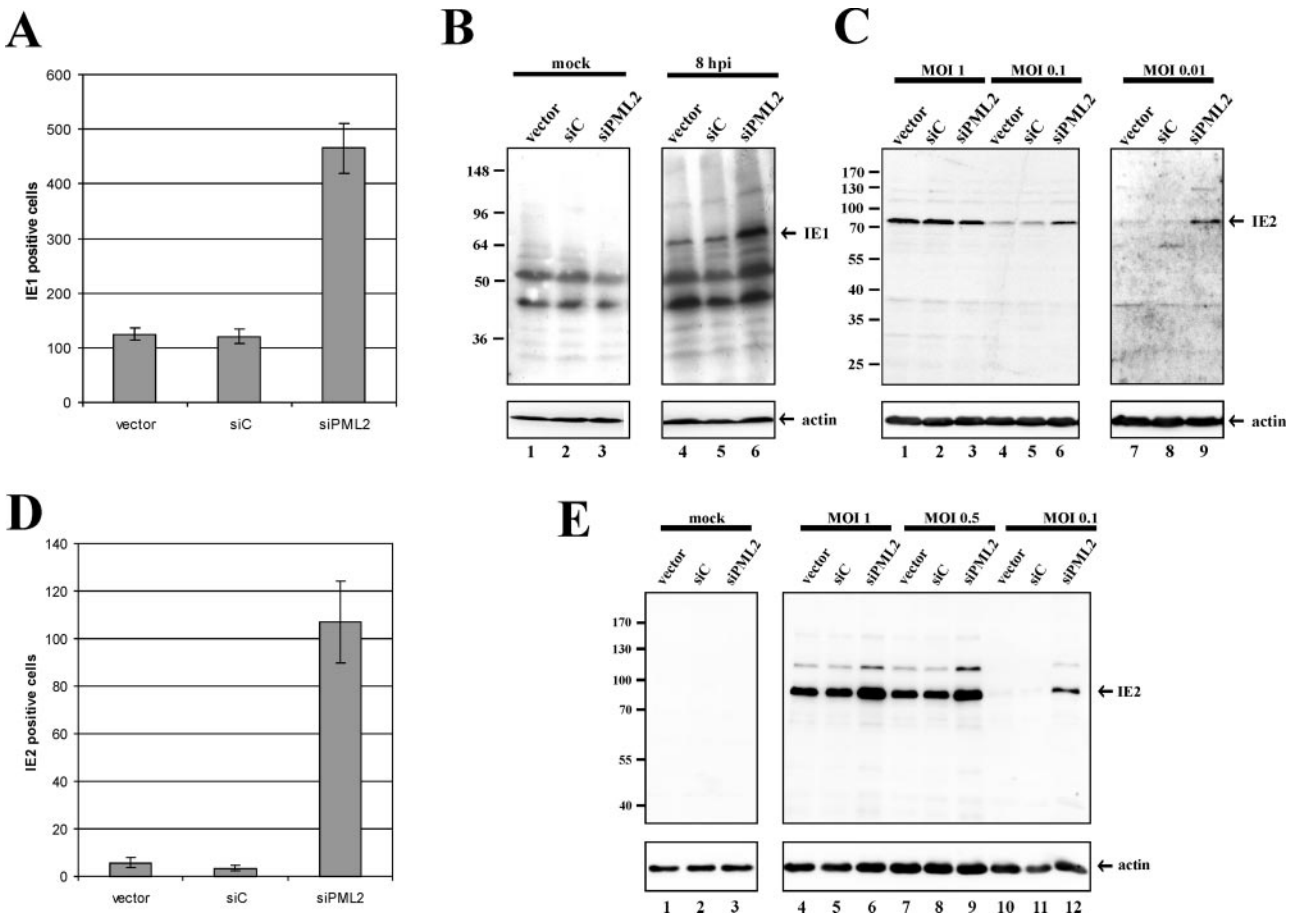

FIG. 9. Analysis of IE gene expression after infection of PML-kd and control cells with wild-type HCMV or the IE1 deletion mutant CR208. (A and D) PML-negative (siPML2) and control (vector, siC) HFFs, grown on coverslips in six-well dishes, were infected with 100 IEU/well of either HCMV strain AD169 (A) or IE1 deletion mutant CR208 (D), respectively. Cells were fixed at 24 hpi, and the number of IE-expressing cells was determined by indirect immunofluorescence analysis using either antibody p63-27 against IE1 (A) or antiserum anti-pHM178 against IE2 (D). (B, C, and E) Western blot analyses of IE gene expression in retrovirally transduced HFFs expressing the respective siRNAs infected with either HCMV AD169 (B and C) or IE1 deletion mutant CR208 (E). (B) HFFs were infected with HCMV AD169 at an MOI of 0.01. Lysates were harvested 8 hpi and analyzed by Western blotting for IE1 gene expression using monoclonal antibody p63-27. (C) HFFs were infected with HCMV AD169 at various MOIs as indicated, and cell extracts were harvested 24 hpi for the detection of the IE protein IE2 (anti-pHM178). (E) HFFs were infected with CR208 at various MOIs as indicated, and cell extracts were harvested 24 hpi for detection of the IE protein IE2 (anti-pHM178). Numbers at left of panels B, C, and E are molecular masses in kilodaltons.

ysis revealed that expression levels of mCh-PML-transduced cells correlated well with PML expression levels of control HFFs, whereas the siPML2 cells, which had been used for the reintroduction of PML, were still negative (Fig. 10C). Finally, the generated mCh-PML cells were infected together with siPML2-expressing HFFs and control HFFs with HCMV followed by the quantification of IE1-positive cells at 24 hpi (Fig. 10D). This clearly shows that the restoration of ND10 structures by expression of mCh-PML reverses the enhanced initiation of IE gene expression as observed in siPML2 HFFs.

DISCUSSION

This study was initiated in order to define the relevance of ND10 domains for HCMV replication. Experimental results of previous studies suggested that ND10 domains may play a pivotal role for the initiation of HCMV IE gene expression. Arguments that could be interpreted in favor of such a proviral role of ND10 were as follows: (i) viral genomes were found to be deposited at the periphery of ND10 (29, 31); (ii) several regulatory proteins of HCMV at least transiently colocalize with PML and other ND10 components (2, 26, 32, 37); (iii) an immediate transcript environment consisting of viral IE transcripts, the IE2 protein, and SC35 domains was reported to form adjacent to ND10-localized HCMV genomes, suggesting that this spatial association is critical for the correct initiation of viral gene expression (31); (iv) only ND10-associated viral genomes were shown to develop into viral replication compartments (4, 48).

As an experimental approach to study the role of ND10 for HCMV replication, we decided to generate primary HFFs with an siRNA-mediated stable knockdown of the PML protein, which is the key component of ND10 (30, 67). We considered HFFs most suitable for our purpose, since these cells are fully permissive for HCMV, thus representing an adequate cell culture system for analysis of HCMV replication. Moreover, they

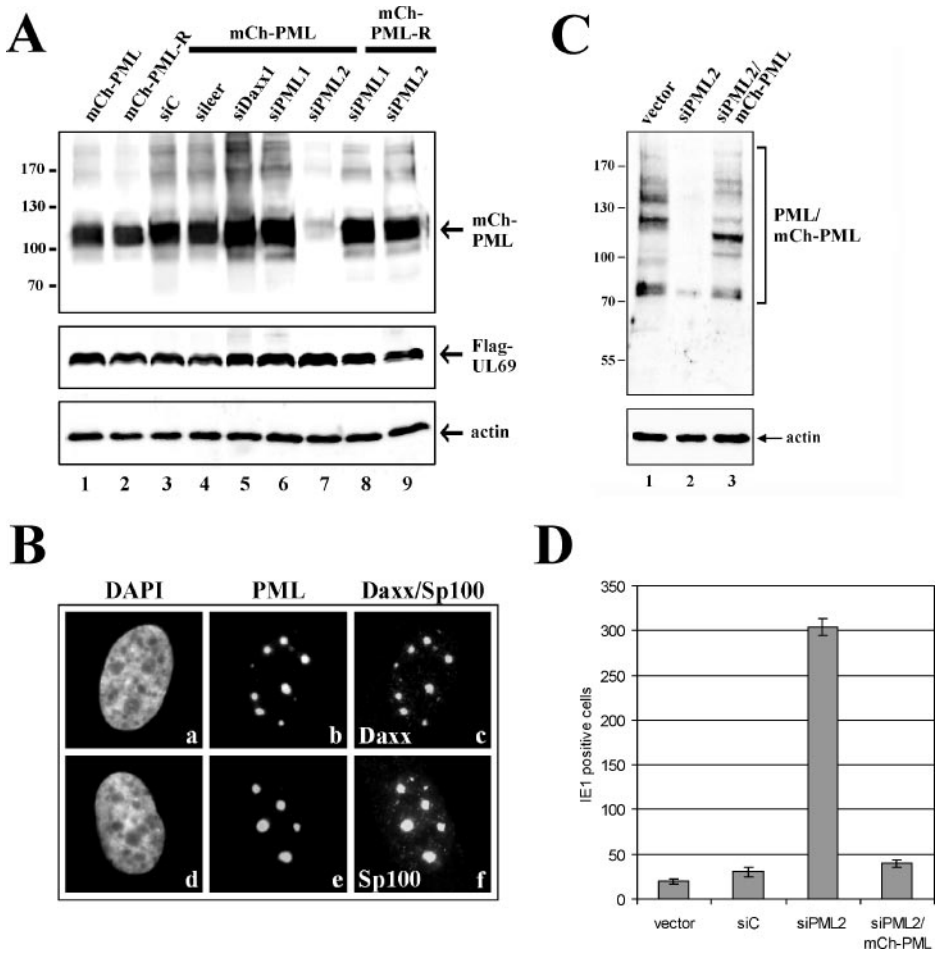

FIG. 10. Reconstitution of PML expression in siPML2 cells. (A) Verification of a PML construct which is resistant against degradation mediated by the PML-siRNA siPML2. HEK293T cells were cotransfected with the respective PML-expressing constructs (mCh-PML comprises the wild-type PML sequence; mCh-PML-R illustrates the degradation-resistant isoform) and a plasmid coding for FLAG-tagged UL69 as well as vectors containing the different siRNA sequences as indicated. Thereafter, cell extracts were analyzed for PML expression using the polyclonal rabbit serum H-238 (upper panel). FLAG-tagged pUL69 was detected by monoclonal antibody anti-FLAG M2 (middle panel). The detection of actin (lower panel) was used as a loading control. (B) Indirect immunofluorescence analysis for detection of PML in siPML2 cells after retroviral gene transfer of the mCh-PML fusion sequence. PML was visualized through autofluorescence of its mCherry moiety. hDaxx and Sp100 were stained using the polyclonal antisera M-117 and H-60, respectively. DAPI, 4′,6′-diamidino-2-phenylindole. (C) Detection of mCh-PML by Western blotting after transduction of siPML2 cells with the mCh-PML expression vector resulting in siPML2/mCh-PML cells. Endogenous PML (lane 1, vector) and reintroduced mCh-PML (lane 3, siPML2/mCh-PML) were detected with the help of the polyclonal antiserum H-238. siPML2 cells, used for transduction with mCh-PML, were analyzed in parallel (lane 2). (D) Analysis of IE gene expression after reintroduction of PML in PML kd cells. The different cell populations as indicated were infected with 25 IEU of HCMV AD169. At 24 hpi the number of IE1-positive cells was determined via indirect immunofluorescence analysis. Numbers at left of panels A and C are molecular masses in kilodaltons.

are characterized by unaltered, genuine ND10 structures, unlike some immortalized cell lines such as the teratocarcinoma and the glioma cell lines NT2 and U373-MG, respectively. For instance, NT2 cells possess abnormal ND10 structures resulting from a lower expression of the defining ND10 component PML, which, in addition, is less extensively modified by the ubiquitin-like protein SUMO-1 (28, 42). Moreover, Sp100, another major ND10 constituent, is completely missing in these cells (28, 30). Although murine PML$^{-/-}$ fibroblasts have been used extensively to study the effect of PML depletion on both cellular and viral regulatory events (e.g., references 6 and 9), we considered this not to be appropriate for our study: while infection of murine cells with HCMV results in the expression of viral IE proteins (38), thus facilitating colocalization studies between viral proteins and ND10 components, an analysis of the overall HCMV replication efficacy is impossible due to the lack of permissiveness. Furthermore, recent results for the retroviral restriction factor TRIM5alpha (59), which is, like PML, a member of the tripartite motif family of proteins (52), suggest a close coevolution of viruses and cellular restriction factors, giving rise to the possibility that murine PML may not function adequately in the context of HCMV infection.

The analysis of the subcellular distribution of HCMV regulatory proteins in PML-depleted cells led to several unanticipated results: after transient expression of IE2 in PML-kd cells, this protein could no longer be found in a dot-like staining pattern as described for normal HFFs (2), indicating that the integrity of ND10 is a prerequisite for this localization.

Surprisingly, however, when PML-kd cells were infected with HCMV, IE2 dots could be observed in the apparent absence of PML and ND10 domains. This suggests that additional viral factors contribute to the dot-like accumulation of IE2 during the viral replication cycle. In contrast, IE1, which transiently colocalizes with ND10 during the first 2 to 3 h after infection of HFFs (2), showed a completely diffuse staining pattern in the absence of PML. This is consistent with earlier reports on a direct protein interaction between IE1 and PML (1). Most importantly, however, we detected an unexpected dynamic of the ND10 components hDaxx and Sp100 elicited by HCMV infection of PML-kd cells: while a dissociation of hDaxx and Sp100 to distinct nuclear sites was observed in uninfected PML-kd cells, HCMV infection resulted in the reorganization of dot-like hDaxx and Sp100 accumulations that colocalized with the viral IE2 protein. This strongly suggests that HCMV infection triggers an active recruitment of these ND10 components to sites of viral nucleoprotein complexes, as was also recently reported in the context of herpes simplex virus infection (18).

Furthermore, these reorganized ND10-like accumulations of hDaxx and Sp100 were only transiently present during the first 2 to 3 h after infection of PML-kd cells with wild-type HCMV; however, they persisted after infection with the IE1 deletion mutant CR208. This implies that the IE1 gene product of HCMV, which was found to be responsible for the disruption of intact ND10 domains (2, 37, 64), also mediates the dispersal of reorganized hDaxx/Sp100 accumulations. Taking into consideration that interference of IE1 with the SUMOylation of PML was described as the mechanism by which IE1 disrupts ND10 (40), we postulate the existence of alternative IE1 mechanisms or targets since we found that IE1 exerts a redistributing activity in the apparent absence of PML.

The results of our analysis of HCMV replication in PML-kd cells clearly argue against an essential role of ND10 structures for the initiation of HCMV replication, since we were not able to detect a diminished replication efficacy. In contrast, increased HCMV replication was observed after infection of PML-kd cells by using alternative experimental approaches. This result was obtained with several independently generated siPML2-expressing cell populations. Furthermore, the fact that the reintroduction of PML into siPML2-expressing cells, which restored ND10 domains, abrogated the phenotype of enhanced HCMV replication strongly argues against the contribution of any off-target RNAi effects.

Further experiments indicated that the augmented replication efficacy of HCMV in PML-deficient cells is a consequence of more cells initiating IE gene expression. We therefore hypothesize that PML contributes to an intrinsic defense mechanism that leads to repression of viral IE gene expression. In this context, it is of note that a stable knockdown of the ND10 component hDaxx in HFFs also results in enhanced replication of wild-type HCMV (N. Tavalai, P. Papior, and T. Stamminger, unpublished results). This is consistent with two recent publications that reported a repressive effect of hDaxx on HCMV IE gene expression, which appears to be counteracted by the viral tegument protein pp71 mediating the degradation of hDaxx (55, 58). Although we noticed lower levels of hDaxx after infection of PML-kd cells with wild-type HCMV (Fig. 5A; compare uninfected and infected cells), hDaxx was still clearly detectable by immunofluorescence (Fig. 5, 6, and 7) or Western blotting (data not shown) experiments, suggesting that pp71 may not be able to induce a complete depletion of hDaxx during HCMV infection. One possible scenario might be that the negative effect of PML on viral IE gene expression is due to the recruitment of hDaxx to the optimal subnuclear site at ND10 where hDaxx then functions as the actual repressor. Alternatively, however, PML and hDaxx may contribute independently or even synergistically to the silencing of IE gene expression, since for both proteins an interaction with chromatin-modifying repressor proteins has been described elsewhere (27, 42, 65). Further experiments aiming at the establishment of HFFs with a double knockdown of PML and hDaxx will help to discriminate between these possibilities.

In addition to pp71, the viral IE1 protein was also implicated in counteracting the repressive effect of ND10 proteins, mediated via the dispersal of ND10 domains (3). Consistent with such a function, we observed a considerably stronger replication enhancement after infection of PML-kd cells with the growth-defective IE1 deletion mutant CR208 (22), which was, in contrast to wild-type HCMV, also detectable under conditions of a high MOI. In a study conducted in parallel it was found that the growth of an ICP0-deficient mutant of HSV-1 was also complemented by depletion of PML from HFFs (19). However, in contrast to HCMV, no effect of PML depletion was observed after infection with wild-type HSV-1. This may relate to the different activities and modes of action of IE1 and ICP0: while ICP0 was shown to induce a proteasome-dependent degradation of PML (16), IE1 seemed to abrogate the SUMOylation of PML, while the overall PML protein levels were not affected (40, 49). Since the SUMOylation of transcription factors often correlates with their repressive activities (20), one may speculate that the abrogation of PML SUMOylation by IE1 may play a role in counteracting the repressive effects of this protein. Alternatively, taking into consideration the recent reports emphasizing the role of chromatin modification for silencing of HCMV IE gene expression (56, 57) as well as the reported interaction of PML with histone deacetylases (65), PML may exert its repressive effect via the induction of transcriptionally repressive chromatin on the HCMV genome. Although the detailed mechanism of PML-mediated repression of viral IE gene expression still remains to be determined, results presented in this study on HCMV and in the accompanying paper on HSV-1 (19) congruently demonstrate that PML contributes to an intrinsic repression mechanism of the cell in herpesvirus gene expression that is counteracted by viral regulatory proteins. Shifting the balance towards cellular repression may constitute a novel principle to inhibit herpesvirus infections.

ACKNOWLEDGMENTS

We thank R. Everett and P. Lischka for helpful discussions and critical reading of the manuscript. Furthermore, we thank R. van Driel (Amsterdam, The Netherlands), R. Greaves (London, United Kingdom), M. Maul (Philadelphia, Pa.), E. Mocarski (Stanford, Calif.), F. Neipel (Erlangen, Germany), M. Nevels (Regensburg, Germany), R. Y. Tsien (San Diego, Calif.), and K. Überla (Bochum, Germany) for providing reagents.

This work was supported by the SFB473, the IZKF Erlangen, and the elite graduate school BIGSS.

REFERENCES

1. **Ahn, J. H., E. J. Brignole III, and G. S. Hayward.** 1998. Disruption of PML subnuclear domains by the acidic IE1 protein of human cytomegalovirus is mediated through interaction with PML and may modulate a RING finger-dependent cryptic transactivator function of PML. Mol. Cell. Biol. **18:**4899–4913.
2. **Ahn, J. H., and G. S. Hayward.** 1997. The major immediate-early proteins IE1 and IE2 of human cytomegalovirus colocalize with and disrupt PML-associated nuclear bodies at very early times in infected permissive cells. J. Virol. **71:**4599–4613.
3. **Ahn, J. H., and G. S. Hayward.** 2000. Disruption of PML-associated nuclear bodies by IE1 correlates with efficient early stages of viral gene expression and DNA replication in human cytomegalovirus infection. Virology **274:**39–55.
4. **Ahn, J. H., W. J. Jang, and G. S. Hayward.** 1999. The human cytomegalovirus IE2 and UL112-113 proteins accumulate in viral DNA replication compartments that initiate from the periphery of promyelocytic leukemia protein-associated nuclear bodies (PODs or ND10). J. Virol. **73:**10458–10471.
5. **Andreoni, M., M. Faircloth, L. Vugler, and W. J. Britt.** 1989. A rapid microneutralization assay for the measurement of neutralizing antibody reactive with human cytomegalovirus. J. Virol. Methods **23:**157–167.
6. **Becker, K. A., L. Florin, C. Sapp, G. G. Maul, and M. Sapp.** 2004. Nuclear localization but not PML protein is required for incorporation of the papillomavirus minor capsid protein L2 into virus-like particles. J. Virol. **78:**1121–1128.
7. **Bieniasz, P. D.** 2004. Intrinsic immunity: a front-line defense against viral attack. Nat. Immunol. **5:**1109–1115.
8. **Boisvert, F. M., M. J. Kruhlak, A. K. Box, M. J. Hendzel, and D. P. Bazett-Jones.** 2001. The transcription coactivator CBP is a dynamic component of the promyelocytic leukemia nuclear body. J. Cell Biol. **152:**1099–1106.
9. **Cairo, S., F. De Falco, M. Pizzo, P. Salomoni, P. P. Pandolfi, and G. Meroni.** 2005. PML interacts with Myc, and Myc target gene expression is altered in PML-null fibroblasts. Oncogene **24:**2195–2203.
10. **Chelbi-Alix, M. K., and H. de The.** 1999. Herpes virus induced proteasome-dependent degradation of the nuclear bodies-associated PML and Sp100 proteins. Oncogene **18:**935–941.
11. **Chelbi-Alix, M. K., L. Pelicano, F. Quignon, M. H. Koken, L. Venturini, M. Stadler, J. Pavlovic, L. Degos, and H. de The.** 1995. Induction of the PML protein by interferons in normal and APL cells. Leukemia **9:**2027–2033.
12. **Chen, L., and J. Chen.** 2003. Daxx silencing sensitizes cells to multiple apoptotic pathways. Mol. Cell. Biol. **23:**7108–7121.
13. **de The, H., C. Lavau, A. Marchio, C. Chomienne, L. Degos, and A. Dejean.** 1991. The PML-RAR alpha fusion mRNA generated by the t(15;17) translocation in acute promyelocytic leukemia encodes a functionally altered RAR. Cell **66:**675–684.
14. **Doucas, V., M. Tini, D. A. Egan, and R. M. Evans.** 1999. Modulation of CREB binding protein function by the promyelocytic (PML) oncoprotein suggests a role for nuclear bodies in hormone signaling. Proc. Natl. Acad. Sci. USA **96:**2627–2632.
15. **Everett, R. D.** 2001. DNA viruses and viral proteins that interact with PML nuclear bodies. Oncogene **20:**7266–7273.
16. **Everett, R. D., P. Freemont, H. Saitoh, M. Dasso, A. Orr, M. Kathoria, and J. Parkinson.** 1998. The disruption of ND10 during herpes simplex virus infection correlates with the Vmw110- and proteasome-dependent loss of several PML isoforms. J. Virol. **72:**6581–6591.
17. **Everett, R. D., P. Lomonte, T. Sternsdorf, R. van Driel, and A. Orr.** 1999. Cell cycle regulation of PML modification and ND10 composition. J. Cell Sci. **112:**4581–4588.
18. **Everett, R. D., and J. Murray.** 2005. ND10 components relocate to sites associated with herpes simplex virus type 1 nucleoprotein complexes during virus infection. J. Virol. **79:**5078–5089.
19. **Everett, R. D., S. Rechter, P. Papior, N. Tavalai, T. Stamminger, and A. Orr.** 2006. PML contributes to a cellular mechanism of repression of herpes simplex virus type 1 infection that is inactivated by ICP0 J. Virol. **80:**7995–8005.
20. **Gill, G.** 2005. Something about SUMO inhibits transcription. Curr. Opin. Genet. Dev. **15:**536–541.
21. **Goddard, A. D., J. Borrow, P. S. Freemont, and E. Solomon.** 1991. Characterization of a zinc finger gene disrupted by the t(15;17) in acute promyelocytic leukemia. Science **254:**1371–1374.
22. **Greaves, R. F., and E. S. Mocarski.** 1998. Defective growth correlates with reduced accumulation of a viral DNA replication protein after low-multiplicity infection by a human cytomegalovirus *ie1* mutant. J. Virol. **72:**366–379.
23. **Guldner, H. H., C. Szostecki, T. Grotzinger, and H. Will.** 1992. IFN enhance expression of Sp100, an autoantigen in primary biliary cirrhosis. J. Immunol. **149:**4067–4073.
24. **Guo, A., P. Salomoni, J. Luo, A. Shih, S. Zhong, W. Gu, and P. P. Pandolfi.** 2000. The function of PML in p53-dependent apoptosis. Nat. Cell Biol. **2:**730–736.
25. **Hofmann, H., S. Floss, and T. Stamminger.** 2000. Covalent modification of the transactivator protein IE2-p86 of human cytomegalovirus by conjugation to the ubiquitin-homologous proteins SUMO-1 and hSMT3b. J. Virol. **74:**2510–2524.
26. **Hofmann, H., H. Sindre, and T. Stamminger.** 2002. Functional interaction between the pp71 protein of human cytomegalovirus and the PML-interacting protein human Daxx. J. Virol. **76:**5769–5783.
27. **Hollenbach, A. D., C. J. McPherson, E. J. Mientjes, R. Iyengar, and G. Grosveld.** 2002. Daxx and histone deacetylase II associate with chromatin through an interaction with core histones and the chromatin-associated protein Dek. J. Cell Sci. **115:**3319–3330.
28. **Hsu, W. L., and R. D. Everett.** 2001. Human neuron-committed teratocarcinoma NT2 cell line has abnormal ND10 structures and is poorly infected by herpes simplex virus type 1. J. Virol. **75:**3819–3831.
29. **Ishov, A. M., and G. G. Maul.** 1996. The periphery of nuclear domain 10 (ND10) as site of DNA virus deposition. J. Cell Biol. **134:**815–826.
30. **Ishov, A. M., A. G. Sotnikov, D. Negorev, O. V. Vladimirova, N. Neff, T. Kamitani, E. T. Yeh, J. F. Strauss III, and G. G. Maul.** 1999. PML is critical for ND10 formation and recruits the PML-interacting protein daxx to this nuclear structure when modified by SUMO-1. J. Cell Biol. **147:**221–234.
31. **Ishov, A. M., R. M. Stenberg, and G. G. Maul.** 1997. Human cytomegalovirus immediate early interaction with host nuclear structures: definition of an immediate transcript environment. J. Cell Biol. **138:**5–16.
32. **Ishov, A. M., O. V. Vladimirova, and G. G. Maul.** 2002. Daxx-mediated accumulation of human cytomegalovirus tegument protein pp71 at ND10 facilitates initiation of viral infection at these nuclear domains. J. Virol. **76:**7705–7712.
33. **Jahn, G., E. Knust, H. Schmolla, T. Sarre, J. A. Nelson, J. K. McDougall, and B. Fleckenstein.** 1984. Predominant immediate-early transcripts of human cytomegalovirus AD 169. J. Virol. **49:**363–370.
34. **Jensen, K., C. Shiels, and P. S. Freemont.** 2001. PML protein isoforms and the RBCC/TRIM motif. Oncogene **20:**7223–7233.
35. **Kakizuka, A., W. H. Miller, Jr., K. Umesono, R. P. Warrell, Jr., S. R. Frankel, V. V. Murty, E. Dmitrovsky, and R. M. Evans.** 1991. Chromosomal translocation t(15;17) in human acute promyelocytic leukemia fuses RAR alpha with a novel putative transcription factor, PML. Cell **66:**663–674.
36. **Kamitani, T., H. P. Nguyen, K. Kito, T. Fukuda-Kamitani, and E. T. Yeh.** 1998. Covalent modification of PML by the sentrin family of ubiquitin-like proteins. J. Biol. Chem. **273:**3117–3120.
37. **Korioth, F., G. G. Maul, B. Plachter, T. Stamminger, and J. Frey.** 1996. The nuclear domain 10 (ND10) is disrupted by the human cytomegalovirus gene product IE1. Exp. Cell Res. **229:**155–158.
38. **Lafemina, R. L., and G. S. Hayward.** 1988. Differences in cell-type-specific blocks to immediate early gene expression and DNA replication of human, simian and murine cytomegalovirus. J. Gen. Virol. **69:**355–374.
39. **LaMorte, V. J., J. A. Dyck, R. L. Ochs, and R. M. Evans.** 1998. Localization of nascent RNA and CREB binding protein with the PML-containing nuclear body. Proc. Natl. Acad. Sci. USA **95:**4991–4996.
40. **Lee, H. R., D. J. Kim, J. M. Lee, C. Y. Choi, B. Y. Ahn, G. S. Hayward, and J. H. Ahn.** 2004. Ability of the human cytomegalovirus IE1 protein to modulate sumoylation of PML correlates with its functional activities in transcriptional regulation and infectivity in cultured fibroblast cells. J. Virol. **78:**6527–6542.
41. **Lehming, N., A. Le Saux, J. Schuller, and M. Ptashne.** 1998. Chromatin components as part of a putative transcriptional repressing complex. Proc. Natl. Acad. Sci. USA **95:**7322–7326.
42. **Li, H., C. Leo, J. Zhu, X. Wu, J. O'Neil, E. J. Park, and J. D. Chen.** 2000. Sequestration and inhibition of Daxx-mediated transcriptional repression by PML. Mol. Cell. Biol. **20:**1784–1796.
43. **Lischka, P., O. Rosorius, E. Trommer, and T. Stamminger.** 2001. A novel transferable nuclear export signal mediates CRM1-independent nucleocytoplasmic shuttling of the human cytomegalovirus transactivator protein pUL69. EMBO J. **20:**7271–7283.
44. **Lischka, P., Z. Toth, M. Thomas, R. Mueller, and T. Stamminger.** 2006. The UL69 transactivator protein of human cytomegalovirus interacts with DEXD/H-Box RNA helicase UAP56 to promote cytoplasmic accumulation of unspliced RNA. Mol. Cell. Biol. **26:**1631–1643.
45. **Lorz, K., H. Hofmann, A. Berndt, N. Tavalai, R. Mueller, U. Schlotzer-Schrehardt, and T. Stamminger.** 2006. Deletion of open reading frame UL26 from the human cytomegalovirus genome results in reduced viral growth, which involves impaired stability of viral particles. J. Virol. **80:**5423–5434.
46. **Marschall, M., M. Freitag, S. Weiler, G. Sorg, and T. Stamminger.** 2000. Recombinant green fluorescent protein-expressing human cytomegalovirus as a tool for screening antiviral agents. Antimicrob. Agents Chemother. **44:**1588–1597.
47. **Maul, G. G.** 1998. Nuclear domain 10, the site of DNA virus transcription and replication. Bioessays **20:**660–667.
48. **Maul, G. G., A. M. Ishov, and R. D. Everett.** 1996. Nuclear domain 10 as preexisting potential replication start sites of herpes simplex virus type-1. Virology **217:**67–75.
49. **Muller, S., and A. Dejean.** 1999. Viral immediate-early proteins abrogate the modification by SUMO-1 of PML and Sp100 proteins, correlating with nuclear body disruption. J. Virol. **73:**5137–5143.

50. **Muller, S., M. J. Matunis, and A. Dejean.** 1998. Conjugation with the ubiquitin-related modifier SUMO-1 regulates the partitioning of PML within the nucleus. EMBO J. **17:**61–70.
51. **Negorev, D., and G. G. Maul.** 2001. Cellular proteins localized at and interacting within ND10/PML nuclear bodies/PODs suggest functions of a nuclear depot. Oncogene **20:**7234–7242.
52. **Nisole, S., J. P. Stoye, and A. Saib.** 2005. TRIM family proteins: retroviral restriction and antiviral defence. Nat. Rev. Microbiol. **3:**799–808.
53. **Paulus, C., S. Krauss, and M. Nevels.** 2006. A human cytomegalovirus antagonist of type I IFN-dependent signal transducer and activator of transcription signaling. Proc. Natl. Acad. Sci. USA **103:**3840–3845.
54. **Plachter, B., W. Britt, R. Vornhagen, T. Stamminger, and G. Jahn.** 1993. Analysis of proteins encoded by IE regions 1 and 2 of human cytomegalovirus using monoclonal antibodies generated against recombinant antigens. Virology **193:**642–652.
55. **Preston, C. M., and M. J. Nicholl.** 2006. Role of the cellular protein hDaxx in human cytomegalovirus immediate-early gene expression. J. Gen. Virol. **87:**1113–1121.
56. **Reeves, M. B., P. J. Lehner, J. G. Sissons, and J. H. Sinclair.** 2005. An in vitro model for the regulation of human cytomegalovirus latency and reactivation in dendritic cells by chromatin remodelling. J. Gen. Virol. **86:**2949–2954.
57. **Reeves, M. B., P. A. MacAry, P. J. Lehner, J. G. Sissons, and J. H. Sinclair.** 2005. Latency, chromatin remodeling, and reactivation of human cytomegalovirus in the dendritic cells of healthy carriers. Proc. Natl. Acad. Sci. USA **102:**4140–4145.
58. **Saffert, R. T., and R. F. Kalejta.** 2006. Inactivating a cellular intrinsic immune defense mediated by Daxx is the mechanism through which the human cytomegalovirus pp71 protein stimulates viral immediate-early gene expression. J. Virol. **80:**3863–3871.
59. **Sawyer, S. L., L. I. Wu, M. Emerman, and H. S. Malik.** 2005. Positive selection of primate TRIM5alpha identifies a critical species-specific retroviral restriction domain. Proc. Natl. Acad. Sci. USA **102:**2832–2837.
60. **Seeler, J. S., A. Marchio, D. Sitterlin, C. Transy, and A. Dejean.** 1998. Interaction of SP100 with HP1 proteins: a link between the promyelocytic leukemia-associated nuclear bodies and the chromatin compartment. Proc. Natl. Acad. Sci. USA **95:**7316–7321.
61. **Shaner, N. C., R. E. Campbell, P. A. Steinbach, B. N. Giepmans, A. E. Palmer, and R. Y. Tsien.** 2004. Improved monomeric red, orange and yellow fluorescent proteins derived from Discosoma sp. red fluorescent protein. Nat. Biotechnol. **22:**1567–1572.
62. **Stuurman, N., A. de Graaf, A. Floore, A. Josso, B. Humbel, L. de Jong, and R. van Driel.** 1992. A monoclonal antibody recognizing nuclear matrix-associated nuclear bodies. J. Cell Sci. **101:**773–784.
63. **Wilcox, K. W., S. Sheriff, A. Isaac, and J. L. Taylor.** 2005. SP100B is a repressor of gene expression. J. Cell Biochem. **95:**352–365.
64. **Wilkinson, G. W., C. Kelly, J. H. Sinclair, and C. Rickards.** 1998. Disruption of PML-associated nuclear bodies mediated by the human cytomegalovirus major immediate early gene product. J. Gen. Virol. **79:**1233–1245.
65. **Wu, W. S., S. Vallian, E. Seto, W. M. Yang, D. Edmondson, S. Roth, and K. S. Chang.** 2001. The growth suppressor PML represses transcription by functionally and physically interacting with histone deacetylases. Mol. Cell. Biol. **21:**2259–2268.
66. **Zhong, S., P. Hu, T. Z. Ye, R. Stan, N. A. Ellis, and P. P. Pandolfi.** 1999. A role for PML and the nuclear body in genomic stability. Oncogene **18:**7941–7947.
67. **Zhong, S., S. Muller, S. Ronchetti, P. S. Freemont, A. Dejean, and P. P. Pandolfi.** 2000. Role of SUMO-1-modified PML in nuclear body formation. Blood **95:**2748–2752.